Review

Materials with ZrCuSiAs-type Structure

Rainer Pöttgen[a] and Dirk Johrendt[b]

[a] Institut für Anorganische und Analytische Chemie, Universität Münster, Corrensstraße 30, 48149 Münster, Germany
[b] Department Chemie und Biochemie, Ludwig-Maximilians-Universität München, Butenandtstraße 5 – 13 (Haus D), 81377 München, Germany

Reprint requests to R. Pöttgen. E-mail: pottgen@uni-muenster.de

Z. Naturforsch. **2008**, *63b,* 1135 – 1148; received July 13, 2008

The discovery of high-temperature superconductivity in the fluoride-doped arsenide oxides *RE*FeAs($O_{1-x}F_x$) (*RE* = early rare earth element) with transition temperatures as high as 55 K has led to a true renaissance in superconductivity research. These arsenide oxides constitute a rather small fraction of a much larger family of compounds with the tetragonal ZrCuSiAs-type structure (space group $P4/nmm$), among them pnictide oxides and fluorides, chalcogenide oxides and fluorides as well as silicide and germanide hydrides. Besides the spectacular superconductivity, these materials have further interesting properties with respect to magnetic ordering, transparent semiconducting behavior or optical properties. The crystal chemical and chemical bonding peculiarities as well as the broadly varying physical properties are reviewed herein.

Key words: Pnictide Oxides, Chalcogenides, Superconductivity, Semiconductors

Introduction

The quaternary silicide arsenides ZrCuSiAs and HfCuSiAs have been reported in 1974 by Johnson and Jeitschko [1]. This structure type is tetragonal, space group *P*4/*nmm*, with two formula units per cell. A similar atomic arrangement has been observed for the ternary silicide $HfCuSi_2$ [2]. These compounds can be considered as filled-up variants of the PbFCl [3 – 5] type structure. The latter derives from the Cu_2Sb type. More than 260 binary and ternary intermetallic compounds with this structure are listed in the Pearson Handbook [6]. Compounds with Cu_2Sb-type structure show different coordination and chemical bonding patterns depending on the size or valence of the constituting elements and have been reviewed by Pearson [7].

Further representatives of the ZrCuSiAs type were described in 1980 by Palazzi *et al.* [8 – 10]. They reported the sulfide oxides LaCuSO and LaAgSO and investigated the silver ion conductivity. Afterwards, many other sulfide and selenide oxides have been reported. This family of compounds has attracted considerable interest in recent years since Ueda and coworkers reported that LaCuSO has an optical band gap of 3.1 eV and exhibits *p*-type electrical conductivity [11, 12]. These materials have potential application as *p*-type transparent semiconductors.

In parallel to the sulfide oxides, several rare earth (*RE*) based pnictide (*Pn*) oxides were reported by the group of Jeitschko [13 – 20]. These compounds were first believed to be ternary pnictides [21], however, careful synthesis yielded pure pnictide oxides. These pnictide oxides can be described with the electron precise formulæ $RE^{3+}T^{2+}Pn^{3-}O^{2-}$ (*T* = late transition metal). Indeed, several of these compounds are transparent with yellow to dark red color, and they have been studied with respect to their optical properties [22, 23]. LaFePO [24, 25] and LaNiPO [26, 27] show superconductivity below 3.2 and 4.3 K, respectively.

Outstanding in this family of compounds are the arsenide oxides which can be doped with fluoride, leading to solid solutions $RETAsO_{1-x}F_x$. This doping induces transitions to superconductivity at comparatively high temperatures, *e. g.* T_C = 26 K for $LaFeAsO_{1-x}F_x$ (x = 0.05 – 0.12) [28]. Most recently an even higher transition temperature of 52 K has been reported for the corresponding praseodymium system [29]. Since that discovery in March 2008, numerous new contributions are published daily on the preprint server of the Cornell University Library (arXiv.org). A short highlight on the recent developments has been published recently [30].

So far more than 150 representatives have been reported for the family of ZrCuSiAs-type compounds

0932–0776 / 08 / 1000–1135 $ 06.00

(Table 1). The latter display a broad crystal chemical variety and different patterns of chemical bonding. The compounds have outstanding physical properties in the fields of magnetism, superconductivity, and transparent semiconductors, and a great potential for applications. The crystal chemical details and the recent developments regarding the physical properties are reviewed herein.

Synthesis

The compounds listed in Table 1 were synthesized *via* different techniques, depending on whether polycrystalline samples or small single crystals were required.

The phosphide oxides were first obtained during syntheses of ternary rare earth (*RE*)-transition metal (*T*)-phosphides using the tin flux technique [21, 31], most likely due to surface contamination of the rare earth filings. Starting materials for these reactions were the elements using a large excess of tin as flux medium and silica tubes as crucible material. Since several of the phosphide oxides have remarkable stability, the tin matrix can be dissolved in moderately diluted (1 : 1) hydrochloric acid. For CeRuPO, crystals with an edge length of 2 mm were obtained in this way [32].

Later, equimolar NaCl/KCl mixtures were used as flux media for crystal growth. In a typical experiment [22], filings of the rare earth element, powder of the transition metal oxide (*e. g.* MnO or ZnO) and powder of red phosphorus were sealed in evacuated silica tubes together with a *ca.* fourfold weight of the flux medium. The temperature profile for the annealing procedure depends on the starting components. In some cases intermetallic precursor compounds can also be used. β-PrZnPO was prepared from $PrZn_2$, Pr_6O_{11}, ZnO, and P in an atomic ratio 11 : 2 : 1 : 23 under salt flux conditions [22]. The salt flux can easily be dissolved in demineralized water. It is thus a good alternative to the tin flux, since no acidic medium is needed for flux dissolution.

Mostly the salt flux technique results in smaller quantities of well-shaped single crystals. For larger amounts of polycrystalline samples a ceramic route can be applied. The rare earth monopnictide (prepared by arc-melting or also *via* a ceramic route) is mixed with the transition metal monoxide and pelletized. The pellets are annealed in evacuated sealed silica tubes up to 1370 K (depending on the constituents). Sometimes regrinding and additional annealing procedures are necessary in order to obtain single phase products. Using this route, *e. g.* LaMnPO [33] and the series *RE*MnSbO and *RE*ZnSbO [34] were obtained.

Table 1. Lattice parameters of the tetragonal compounds with ZrCuSiAs-type structure.

Compound	*a* (pm)	*c* (pm)	*V* (nm^3)	Reference
Phosphide oxides				
LaMnPO	405.78	884.36	0.1456	[33]
	405.4(1)	883.4(4)	0.1452	[18]
CeMnPO	402.0(1)	874.2(3)	0.1413	[18]
PrMnPO	400.6(1)	870.7(2)	0.1397	[18]
NdMnPO	398.9(1)	867.4(1)	0.1380	[18]
SmMnPO	396.0(1)	859.0(3)	0.1347	[18]
GdMnPO	393.3(1)	851.0(1)	0.1316	[18]
TbMnPO	392.0(1)	848.5(4)	0.1304	[18]
DyMnPO	390.4(1)	846.9(4)	0.1291	[18]
LaFePO	396.4(1)	851.2(3)	0.1338	[25]
	395.70(9)	850.7(4)	0.1332	[14]
	396.10(1)	851.58(2)	0.1336	[87]
	396.2	851.1	0.1336	[52]
	396.307(4)	850.87(1)	0.1336	[47]
CeFePO	391.9(1)	832.7(3)	0.1279	[14]
	391.9(3)	833.0(5)	0.1279	[48]
PrFePO	391.13(6)	834.5(2)	0.1277	[14]
NdFePO	389.95(5)	830.2(3)	0.1262	[14]
'SmFeP'	388.03(6)	819.8(4)	0.1234	[21]
SmFePO	387.8(1)	820.5(1)	0.1234	[14]
GdFePO	386.1(3)	812.3(7)	0.1211	[14]
LaCoPO	396.78(9)	837.9(3)	0.1319	[14]
	396.81(9)	837.79(1)	0.1319	[46]
CeCoPO	392.13(7)	821.9(4)	0.1264	[14]
'PrCoP'	392.29(5)	821.5(2)	0.1264	[21]
PrCoPO	392.24(8)	822.4(2)	0.1265	[14]
'NdCoP'	390.44(9)	817.3(3)	0.1246	[21]
NdCoPO	390.84(5)	817.2(2)	0.1248	[14]
'SmCoP'	388.45(4)	808.5(1)	0.1220	[21]
SmCoPO	388.17(7)	807.3(2)	0.1216	[14]
LaNiPO	404.53(1)	810.54(3)	0.1326	[27]
	404.61(8)	810.0(7)	0.1326	[26]
ThCuPO	389.43(4)	828.3(1)	0.1256	[15]
UCuPO	379.3(1)	823.3(2)	0.1184	[13]
LaZnPO	404.0(1)	890.8(2)	0.1454	[19]
	402.759(14)	887.105(12)	0.1439	[64]
	404.109(1)	890.486(3)	0.1454	[50]
α-CeZnPO	401.3(1)	882.4(2)	0.1421	[19]
	401.08(9)	882.0(4)	0.1419	[22]
α-PrZnPO	399.3(2)	877.2(7)	0.1399	[22]
ThAgPO	396.6(1)	878.6(3)	0.1382	[16, 49]
LaCdPO	417.2(2)	906.7(6)	0.1578	[78]
LaRuPO	404.8(2)	841.0(4)	0.1378	[51]
	404.7(1)	840.6(1)	0.1377	[14]
CeRuPO	402.8(1)	825.6(2)	0.1340	[51]
	402.7(3)	826(1)	0.1340	[32]
	402.6(1)	825.6(2)	0.1338	[14]
PrRuPO	401.8(1)	817.4(3)	0.1320	[14]
NdRuPO	400.86(5)	816.7(2)	0.1312	[14]
SmRuPO	399.35(5)	805.8(2)	0.1285	[14]
GdRuPO	397.9(1)	797.4(2)	0.1262	[14]
TbRuPO	397.1(1)	792.7(2)	0.1250	[16, 49]

Table 1 (continued).

Compound	*a* (pm)	*c* (pm)	*V* (nm^3)	Reference
DyRuPO	396.25(1)	787.2(2)	0.1236	[16, 49]
LaOsPO	404.8(3)	840.8(6)	0.1378	[16, 49]
CeOsPO	402.8(1)	828.7(3)	0.1345	[16, 49]
	403.1(1)	828.6(3)	0.1346	[51]
PrOsPO	402.06(6)	824.1(2)	0.1332	[16, 49]
NdOsPO	401.01(1)	819.2(2)	0.1317	[16, 49]
SmOsPO	399.6(1)	806.9(3)	0.1288	[16, 49]
Phosphide fluorides				
BaMnPF	417.93(2)	950.40(5)	0.1660	[35]
SrZnPF	403.15(1)	901.14(6)	0.1465	[35]
BaZnPF	415.637(3)	945.74(1)	0.1634	[36]
EuMnPF	402.9(1)	894.9(1)	0.1453	[66]
Phosphides and arsenides				
ZrCuSiP	356.71(1)	944.69(4)	0.1202	[67]
ZrCuSiAs	367.36(2)	957.12(9)	0.1292	[1]
HfCuSiAs	363.4(1)	960.1(1)	0.1268	[1]
Arsenide oxides				
YMnAsO	395.7(1)	875.0(6)	0.1370	[18]
LaMnAsO	412.4(1)	903.0(5)	0.1536	[18]
CeMnAsO	408.6(1)	895.6(2)	0.1495	[18]
PrMnAsO	406.7(1)	891.9(3)	0.1475	[18]
NdMnAsO	404.9(2)	889.3(1)	0.1458	[18]
SmMnAsO	402.0(1)	882.9(3)	0.1427	[18]
GdMnAsO	398.9(1)	880.5(3)	0.1401	[18]
TbMnAsO	397.8(1)	874.3(4)	0.1384	[18]
DyMnAsO	395.9(1)	872.7(4)	0.1368	[18]
UMnAsO	386.9(1)	852.5(2)	0.1276	[18]
LaFeAsO	403.552(8)	873.93(2)	0.1423	[28]
	403.2	872.6	0.1419	[62]
	403.007(9)	873.68(2)	0.1419	[55]
	403.397(4)	874.49(4)	0.1423	[63]
	403.8(1)	875.3(6)	0.1427	[20]
	403.268(1)	874.111(4)	0.1422	[54]
$LaFeAsO_{1-x}F_x$	402.4	871.7	0.1412	[57]
	403.0(1)	870.6(2)	0.1414	[58]
CeFeAsO	400.0(1)	865.5(1)	0.1385	[20]
	399.6	864.8	0.1381	[59]
PrFeAsO	398.5(1)	859.5(3)	0.1365	[20]
$PrFeAsO_{1-x}F_x$	396.7(1)	856.1(3)	0.1347	[29]
NdFeAsO	396.5(1)	857.5(2)	0.1348	[20]
SmFeAsO	394.0(1)	849.6(3)	0.1319	[20]
	393.3(5)	849.5(4)	0.1314	[61]
	394.0	849.6	0.1319	[56]
GdFeAsO	391.5(1)	843.5(4)	0.1293	[20]
$GdFeAsO_{1-x}F_x$	400.1	865.0	0.1385	[60]
LaCoAsO	405.4(1)	847.2(3)	0.1392	[20]
	405.26(1)	846.20(4)	0.1390	[46]
CeCoAsO	401.5(1)	836.4(2)	0.1348	[20]
PrCoAsO	400.5(1)	834.4(2)	0.1338	[20]
NdCoAsO	398.2(1)	831.7(4)	0.1319	[20]
LaNiAsO	412.309(1)	818.848(6)	0.1392	[53]
ThCuAsO	396.14(5)	844.0(1)	0.1324	[15]
YZnAsO	394.3(1)	884.3(3)	0.1375	[19]
LaZnAsO	409.5(1)	906.8(3)	0.1521	[19]
	410.492(13)	908.178(47)	0.1530	[64]
CeZnAsO	406.9(1)	899.5(3)	0.1489	[19]
	406.79(5)	899.8(1)	0.1489	[64]

Table 1 (continued).

Compound	*a* (pm)	*c* (pm)	*V* (nm^3)	Reference
PrZnAsO	404.7(1)	896.3(1)	0.1468	[19]
	404.77(2)	896.6(2)	0.1469	[64]
NdZnAsO	403.0(1)	894.9(4)	0.1453	[19]
	402.95(6)	895.2(1)	0.1454	[64]
SmZnAsO	400.3(1)	890.3(2)	0.1427	[19]
GdZnAsO	397.6(1)	889.4(3)	0.1406	[19]
TbZnAsO	395.7(1)	884.1(2)	0.1384	[19]
DyZnAsO	394.7(1)	883.8(1)	0.1377	[19]
LaCdAsO	412.9(2)	923.0(3)	0.1643	[78]
CeCdAsO	419.1(1)	917.1(4)	0.1611	[78]
PrCdAsO	417.2(1)	913.6(4)	0.1590	[78]
NdCdAsO	415.1(1)	912.3(5)	0.1572	[78]
(Nd, Sm)CdAsO	414.7(2)	912.5(6)	0.1569	[78]
LaRuAsO	411.9(1)	848.8(1)	0.1440	[20]
CeRuAsO	409.6(1)	838.0(3)	0.1406	[20]
PrRuAsO	408.5(1)	833.7(1)	0.1391	[20]
NdRuAsO	407.9(1)	829.2(2)	0.1380	[20]
SmRuAsO	405.0(2)	819.1(7)	0.1343	[20]
GdRuAsO	403.9(1)	811.8(6)	0.1324	[20]
TbRuAsO	402.7(1)	807.8(1)	0.1310	[20]
DyRuAsO	402.2(2)	805.0(3)	0.1302	[20]
Antimonide oxides				
LaMnSbO	423.95(7)	955.5(2)	0.1717	[34]
	424.2(1)	955.7(2)	0.1720	[18]
CeMnSbO	420.8(1)	950.7(1)	0.1683	[34]
	421.8(1)	951.7(2)	0.1693	[18]
PrMnSbO	418.8(1)	947.2(3)	0.1661	[34]
	418.7(1)	946.0(1)	0.1658	[18]
NdMnSbO	416.6(1)	947.1(3)	0.1644	[34]
	416.5(1)	946.2(2)	0.1641	[18]
SmMnSbO	413.1(1)	942.3(1)	0.1608	[34]
	413.5(1)	941.8(2)	0.1610	[18]
GdMnSbO	410.0(1)	942.1(2)	0.1584	[34]
	409.0(1)	941.0(1)	0.1574	[18]
TbMnSbO	408.3(1)	939.2(6)	0.1566	[34]
LaZnSbO	422.67(6)	953.8(2)	0.1704	[34]
	422.62(2)	953.77(6)	0.1704	[17]
	422.604(7)	953.691(24)	0.1703	[64]
CeZnSbO	419.9(1)	948.7(2)	0.1673	[34]
	419.76(4)	947.4(1)	0.1669	[17]
	419.66(2)	947.96(4)	0.1669	[64]
PrZnSbO	418.79(8)	946.7(5)	0.1660	[34]
	417.63(4)	945.1(1)	0.1648	[17]
NdZnSbO	415.9(1)	945.4(4)	0.1635	[34]
	415.81(2)	944.95(5)	0.1634	[17]
	415.78(2)	944.33(5)	0.1632	[64]
SmZnSbO	412.80(2)	940.16(6)	0.1602	[17]
Antimonide fluorides				
BaZnSbF	443.84(2)	977.89(6)	0.1926	[35]
Bismuthide oxides				
$LaNiBiO_{0.8}$	407.3	930.1	0.1543	[65]
Sulfide oxides				
BiCuSO	387.05(5)	856.1(1)	0.1283	[82]
	387.08(8)	855.8(1)	0.1282	[43]
	386.91(1)	856.02(4)	0.1281	[44]
LaCuSO	399.9(1)	853(4)	0.1364	[10]
	399.484(2)	851.254(5)	0.1358	[85]

Table 1 (continued).

Compound	a (pm)	c (pm)	V (nm^3)	Reference
	399.5	851.0	0.1358	[42]
	399.6	851.7	0.1360	[86]
	399.38(2)	852.15(4)	0.1359	[44]
	399.625(4)	851.743(9)	0.1360	[79]
CeCuSO	392.3	833.3	0.1282	[83]
	392.28(1)	834.75(3)	0.1285	[79]
$CeCu_{1-x}SO$	391.9(1)	843.2(3)	0.1295	[39]
$CeCu_{0.95}SO$	391.7(2)	841.2(3)	0.1290	[39]
$CeCu_{0.90}SO$	391.8(1)	839.4(5)	0.1288	[39]
$CeCu_{0.85}SO$	391.1(1)	836.5(3)	0.1279	[39]
$CeCu_{0.809}SO$	391.42(3)	829.80(10)	0.1271	[40]
$CeCu_{0.762}SO$	390.72(3)	828.34(10)	0.1265	[40]
PrCuSO	394.19(4)	843.98(9)	0.1311	[84]
	393.9(1)	843.8(3)	0.1309	[39]
	394.1	843.8	0.1311	[86]
	394.148(9)	843.76(1)	0.1311	[79]
NdCuSO	390.3(5)	848.0(1)	0.1292	[81]
	391.8(1)	843.4(6)	0.1295	[39]
	392	842.8	0.1295	[86]
	391.96(1)	842.82(2)	0.1295	[79]
SmCuSO	385.4(3)	844.2(7)	0.1254	[81]
	388.7(3)	838.5(7)	0.1267	[39]
EuCuSO	387.4(2)	837.9(6)	0.1258	[39]
LaAgSO	405.0(2)	903.9(3)	0.1483	[9]
	406.6(1)	909.5(1)	0.1504	[8]
$CeAg_{0.777}SO$	392.56(3)	899.43(9)	0.1386	[40]
$CeAg_{0.763}SO$	392.30(3)	901.30(8)	0.1387	[40]
Sulfide fluorides				
SrCuFS	395.70(2)	865.98(7)	0.1356	[73]
BaCuSF	412.30(1)	903.27(2)	0.1535	[72]
EuCuSF	394.74(3)	864.25(6)	0.1347	[45]
Selenide oxides				
BiCuSeO	392.13(1)	891.33(5)	0.1371	[82]
	392.87(1)	892.91(2)	0.1378	[44]
YCuSeO	389.89(1)	863.20(2)	0.1312	[38]
	387.89(1)	873.11(5)	0.1314	[86]
	388.09(1)	874.34(1)	0.1317	[77]
LaCuSeO	408.98(2)	893.75(3)	0.1495	[38]
	406.5(1)	879.2(1)	0.1453	[39]
	406.7	879.8	0.1455	[86]
	406.70(1)	880.06(8)	0.1456	[44]
	406.65(3)	881.19(2)	0.1457	[77]
CeCuSeO	401.85(15)	871.14(14)	0.1407	[77]
$CeCu_{1-x}SeO$	398.8(1)	875.0(4)	0.1391	[39]
$CeCu_{0.95}SeO$	398.8(1)	868.7(3)	0.1382	[39]
$CeCu_{0.90}SeO$	398.3(2)	868.6(5)	0.1377	[39]
$CeCu_{0.85}SeO$	397.7(1)	866.7(3)	0.1370	[39]
$CeCu_{0.80}SeO$	397.9(2)	864.9(4)	0.1369	[39]
PrCuSeO	400.4(3)	873.3(4)	0.1400	[39]
NdCuSeO	398.6(1)	883.3(4)	0.1403	[82]
	398.54(4)	874.67(2)	0.1389	[77]
SmCuSeO	395.12(1)	871.57(2)	0.1361	[38]
	395.63(1)	871.64(1)	0.1364	[77]
EuCuSeO	393.6(1)	871.6(4)	0.1350	[39]
GdCuSeO	392.73(1)	867.72(2)	0.1338	[38]
	391.86(2)	872.3(5)	0.1339	[76]
	392.06(8)	874.3(2)	0.1344	[82]
	392.08(5)	870.68(1)	0.1338	[77]

Table 1 (continued).

Compound	a (pm)	c (pm)	V (nm^3)	Reference
TbCuSeO	390.2(1)	870.5(2)	0.1325	[39]
	390.58(4)	871.71(1)	0.1330	[77]
DyCuSeO	388.54(2)	870.1(4)	0.1314	[76]
	388.65(6)	870.9(1)	0.1316	[82]
	389.57(2)	875.29(2)	0.1328	[77]
HoCuSeO	386.6(2)	868.5(7)	0.1298	[76]
	387.0(1)	871.1(2)	0.1304	[39]
	387.25(3)	870.28(1)	0.1305	[77]
ErCuSeO	385.6(1)	871.1(2)	0.1295	[39]
LaAgSeO	412.5(1)	930.0(2)	0.1582	[80]
CeAgSeO	400.9(2)	934.7(5)	0.1502	[80]
PrAgSeO	406.9(1)	929.3(4)	0.1539	[80]
NdAgSeO	404.1(1)	931.3(4)	0.1521	[80]
$Nd_{0.6}Sm_{0.4}AgSeO$	402.8(3)	930.1(11)	0.1509	[80]
Telluride oxides				
BiCuTeO	404.11(2)	952.37(5)	0.1555	[44]
LaCuTeO	417.92(1)	933.17(3)	0.1630	[81]
	418.15(3)	934.17(7)	0.1633	[75]
	417.75(5)	932.60(16)	0.1628	[41]
	418.08(2)	934.41(8)	0.1633	[44]
CeCuTeO	414.97(3)	930.90(10)	0.1603	[41]
	409.7(1)	930.3(3)	0.1562	[39]
PrCuTeO	412.1(1)	929.9(5)	0.1578	[39]
NdCuTeO	410.56(9)	933.2(4)	0.1573	[41]
	409.7(1)	931.8(4)	0.1564	[39]
LaAgTeO	423.3(2)	984.1(5)	0.1763	[80]
Selenide fluorides				
BaCuSeF	423.91(1)	912.17(2)	0.1639	[72]
SmCuSeF	405.81(3)	881.32(7)	0.1451	[74]
Hydrides				
CeMnSiH	407.7	791.7	0.1316	[69]
CeMnGeH	414.1	794.0	0.1362	[69]
	414.08(2)	794.01(3)	0.1361	[71]
CeFeSiH	399.4(2)	781.0(4)	0.1246	[71]
CeCoSiH	395.5(2)	786.1(3)	0.1230	[37]
LaCoGeH	406.3(2)	791.2(3)	0.1306	[68]
CeCoGeH	404.0(2)	773.5(4)	0.1262	[68]
LaRuSiH	420.2(1)	772.1(1)	0.1363	[70]
CeRuSiH	417.98(5)	751.20(7)	0.1312	[70]
CeRuSiH	417.77(1)	750.72(1)	0.1302	[88]

Various doping methods for investigating the superconducting behavior with higher- or lower-valent metal cations have been introduced. Typical sources are zirconium metal or Ca_3P_2. The doping with fluoride can be performed *via* FeF_3 or the rare earth fluorides. Besides the transition metal oxides the rare earth metal oxides can also be used as oxygen sources.

The pnictide fluorides were synthesized with the difluorides of the alkaline earth (*AE*) elements as a fluoride source according to the general equation $AEF_2 + AE + 2T + 2Pn \rightarrow 2AETPn$F. Sealed evacuated silica tubes were used as crucibles, and a special annealing sequence with a maximum temperature of 1170 K [35]

was applied. The reaction mixtures were first heated at 770 K in order to account for the vapor pressure of the pnictogen in the initial reaction step. BaZnPF can also be synthesized *via* a metathesis reaction according to NaZnP + BaFCl → BaZnPF + NaCl [36]. The pnictide fluorides are stable in air.

The ZrCuSiAs-type hydrides were synthesized starting from the ternary intermetallic compounds. The latter can be obtained *via* arc-melting and subsequent annealing. As an example we give the synthesis conditions for CeCoSiH [37]. A CeCoSi ingot is first annealed under vacuum at 523 K for 12 h and then exposed to 4 MPa hydrogen gas at the same temperature. The hydrogenation procedure always induces a decrepitation of the starting ingot into small grains, and the resulting hydrides are stable in air.

The chalcogenide oxides were mostly prepared by classical solid state reactions. Starting materials were rare earth metals, rare earth sesquioxides, powders of the chalcogen, and copper powder [38]. The educts were all thoroughly mixed and ground to powders, pressed into pellets and annealed in evacuated silica tubes. The maximum annealing temperature depends on the chalcogen component. Longer reaction times up to 15 d and intermediate grindings may be necessary. In some cases, also freshly prepared copper(II) oxide (prepared by heating $Cu(NO_3)_2 \cdot 2H_2O$ in air) can be used as an oxygen source [39]. Alternatively, also mixtures of La_2S_3, Cu_2S, and La_2O_3 can be used with alumina as crucible material. SrS is a suitable precursor for the synthesis of doped samples like $La_{1-x}Sr_xCuSO$. Thin films of LaCuSO, and related sulfide oxides can effectively be prepared by radiofrequency sputtering [11]. Crystal growth of the CeAgSO [40] and *RE*CuTeO (*RE* = La, Ce, Nd) [41] compounds can be ameliorated using small amounts of KCl and KI as flux reagents. Crystals of LaCuSO were obtained by heating a polycrystalline powder in an iodine atmosphere at 1373 K [42].

Besides the classical solid state reactions, the sulfide oxides are also accessible through hydrothermal reactions at significantly lower temperatures [43]. BiCuSO was obtained from Bi_2O_3, Cu_2O, and Na_2S in a Teflon-lined pressure vessel using water as solvent. In contrast to the solid state reaction, the maximum temperature for the hydrothermal reaction was only 520 K. Another approach for the synthesis of BiCuSO is the use of reactive precursor compounds. Hiramatsu *et al.* [44] used freshly prepared $BiCu_3S_3$ (obtained from Bi_2S_3 and Cu_2S under a flow of a 5 % H_2S and 95 % H_2 gas mixture at 570 K) and α-Bi_2O_3 for the solid state reaction.

Platinum is a useful container material for the synthesis of fluoride sulfides. EuCuSF [45] was obtained from Eu, EuF_3, Cu and S in 2 : 1 : 3 : 3 molar ratios in a NaCl flux in a sealed platinum ampoule at 1120 K. For the synthesis of the BaCu*Q*F samples (*Q* = S, Se), CuS, CuSe, BaS, BaSe, Cu, and BaF_2 were used as starting reagents for the solid state reactions [38] at 720 K.

Crystal Chemistry

The ZrCuSiAs-type structure has more than 150 representatives. In Table 1 we have listed the basic crystallographic data of these compounds classified according to their *p*-element components [1, 8 – 10, 13 – 29, 32 – 88]. As emphasized in Fig. 1, these compounds are composed of two different layers, both with tetrahedral coordination patterns. The transition metal atoms have tetrahedral coordination by a heavier chalcogen or pnicogen atom, while the silicon, oxygen, and fluorine atoms fill the tetrahedral voids left by the electropositive elements. The different tetrahedral layers are stacked in an AB AB sequence. As emphasized below, chemical bonding within the layers has predominantly covalent character, while the interlayer bonding is of an ionic type.

Repeatedly, these materials have been classified as layer compounds; however, they do not meet the requirements for a layer structure, *i. e.* they have no van der Waals gap with weak interlayer bonding (such layers can easily be disrupted mechanically leading to softness of the material) like in graphite or molybdenum sulfide.

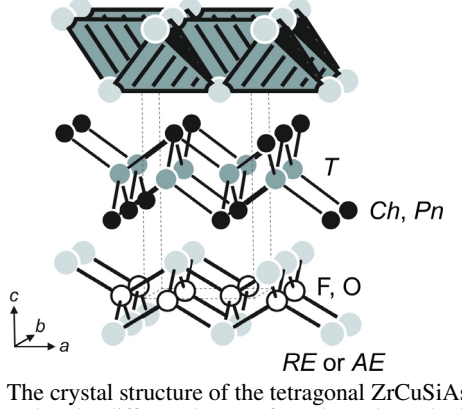

Fig. 1. The crystal structure of the tetragonal ZrCuSiAs-type compounds. The different layers of condensed tetrahedra are emphasized. For details see text.

Most of the ZrCuSiAs-type compounds are stable over a wide range of temperatures. So far, dimorphism with a rhombohedral NdZnPO type high-temperature modification has only been observed for CeZnPO and PrZnPO [19, 22].

The oxides, fluorides, and the recently reported hydrides in this family of compounds can be described, to a first approximation, with simple ionic formula splittings, *e. g.* $Pr^{3+}Zn^{2+}P^{3-}O^{2-}$, $La^{3+}Ag^{+}S^{2-}O^{2-}$ or $Ce^{3+}Fe^{2+}Si^{4-}H^{-}$. This description is certainly justified, since several phosphides and sulfides are transparent, while some arsenides, antimonides and the hydrides are black. In all cases, the rare earth-containing layers are positively, and the transition metal-containing layers negatively charged according to $[Pr^{3+}O^{2-}]^{+}[Zn^{2+}P^{3-}]^{-}$, $[La^{3+}O^{2-}]^{+}[Ag^{+}S^{2-}]^{-}$, $[Th^{4+}O^{2-}]^{2+}[Ag^{+}P^{3-}]^{2-}$, or $[Ce^{3+}H^{-}]^{2+}[Fe^{2+}Si^{4-}]^{2-}$, enabling carrier flows between the layers.

Although a precise formula splitting is possible for the ZrCuSiAs-type compounds, several examples show significant defects on the transition metal site. If such defects occur, the systems switch to metallicity. Prominent examples are $BiCu_{0.97}SO$, $BiCu_{0.97}SeO$, $LaCu_{0.96}SO$, $LaCu_{0.94}SeO$, $LaCu_{0.96}TeO$ [44] and the series $CeCu_{1-x}SO$ [40], $CeCu_{1-x}SeO$ [39], and $CeAg_{1-x}SO$ [40]. In the latter case, the different formation of defects has a drastic influence on the magnetic behavior (*vide infra*).

An important parameter for the physical properties is the interlayer distance between the two layer types. Hiramatsu *et al*. [44] have studied the crystal structures of the two series LaCu*Ch*O and BiCu*Ch*O (*Ch* = S, Se, Te) in order to get reliable values for the interatomic distances. The *c* parameters strongly increase from 856 (BiCuSO) to 952 pm (BiCuTeO) and from 852 (LaCuSO) to 934 pm (LaCuTeO). Consequently one observes significantly different distances and bond angles within the square prisms around the lanthanum (bismuth) atoms and within the $CuCh_4$ tetrahedra.

Chemical Bonding

The two-dimensional nature of the ZrCuSiAs-type structure reflects the chemical bonding pattern. Bonding interactions between atoms of different electronegativities are responsible for a more or less pronounced ionic character of the ZrCuSiAs-type compounds. The bonding scenario can be subdivided into three main aspects: Firstly, all compounds are stabilized by electron transfer between the layers according to, for instance, $[LaO]^{+}[FeAs]^{-}$. Secondly, the bonds within the transition metal layers [Fe–As] have more covalent character than those inside the oxide layers [La–O] and between the layers [La–As], which are largely ionic. This is in agreement with an analysis of the chemical bonding in the ZrCuSiAs-type hydride CeCoSiH, which showed the by far strongest covalent Co–Si bonds inside the [CoSi] layers [37]. The third point concerns direct metal-metal interactions between the transition metals, which may become significantly bonding if the *d* shell is only partially filled.

The charge transfer between the layers is of course smaller than in the purely ionic picture. A Bader analysis of the charge distribution in LaOFeP resulted in $[LaO]^{0.36+}[FeP]^{0.36-}$ [89]. Electronic, optical and magnetic properties strongly depend on the character of the electronic states close to the Fermi level. In semiconducting closed shell systems like *RE*ZnPO, the energy gap occurs between the P-3*p* valence band and the conduction band made up of Zn-4*s*/P-3*p* antibonding states. The latter slightly hybridize with the 5*d* and 4*f* orbitals of the *RE* atoms, which leads to subtle nuances of the gap and thus to different colors of the compounds [23]. But the band gap is also affected by interactions between the transition metal (d^{10}) atoms, as discussed for the *RE*Cu*X*O (*X* = S, Se) compounds [86]. A comparable scenario was reported for the sulfide oxide LaCuSO, which is a transparent *p*-type semiconductor with a band gap around 3 eV [90]. Band structure calculations and photoemission experiments have shown consistently that the valence band mainly consists of Cu states, hybridized with S-3*p* orbitals (Cu–S antibonding). The Cu-3*d* states are remarkably broadened probably due to direct Cu–Cu interactions, and thus the band gap is strongly affected by the metal-metal distances. Of course, the gap also depends strongly on the energy of the lowest conduction band levels, which are the Cu-4*s* in LaCuSO and the Zn-4*s* in *RE*ZnPO. Thus, the gap is mainly determined by the [CuS] or [ZnP] layers in LaCuSO and *RE*ZnPO, respectively. Consequently, a much smaller gap was observed in BiCuOS (1.1 eV), where the conduction band is formed by the lower lying Bi-6*p* orbitals [44].

Metallic properties arise if the transition metal *d* shell is partially occupied. In this case, the Fermi level is always dominated by the *d* orbitals [89, 91], more or less hybridized with the *p* orbitals of the particular main group element. According to the two-

dimensional character, especially the $d_{x^2-y^2}$ and d_{xy} orbitals of the metal atoms play a key role for the magnetic and presumably also the superconducting properties, because they generate flat bands leading to special Fermi surface features [89, 92]. The band filling puts these orbitals close to the Fermi level in the cases of LaFeAsO and LaFePO, but not of LaNiPO or LaNiAsO. This may be one reason for the fact that superconductivity occurs only at very low temperatures in the nickel compounds ($T_C < 4$ K) and could not be increased by doping. From this it is assumed that the pairing mechanisms of phosphide oxide and arsenide oxide superconductors are different [92].

The electronic structures and the influence of doping on the Fermi surface and magnetism of LaFeAsO and related compounds were intensively studied by theoretical methods [91, 93]. The calculated magnetic moments are mostly found too large ($\sim 1\ \mu_B$) in comparison with the experimental values ($\sim 0.35\ \mu_B$) [94], which indicates that the theoretical description of the new materials is not yet under control. Most results support the view that spin fluctuations play an important rule for the pairing, but the exact mechanism remains to be seen in the future. However, this field is rapidly growing and outside the scope of this review.

Physical Properties

Magnetic behavior

Although a huge number of ZrCuSiAs-type compounds are known, only few of them have been studied with respect to their magnetic properties. The basic magnetic data are summarized in Table 2. The investigated lanthanum compounds LaZnPO, LaZnAsO, LaZnSbO, LaCuSO, and LaCuTeO are all diamagnetic with only weak upturns of the susceptibilities at low temperatures, indicating only trace amounts of paramagnetic impurities. These data underline the closed-shell d^{10} character of copper in the two chalcogenides. Different behavior has been observed for LaMnPO [33], where the manganese ions (Mn^{2+} d^5) carry a magnetic moment and reveal ferromagnetic ordering at 320 K.

Susceptibility measurements of these diamagnets or Pauli paramagnets may be affected by ferromagnetic or antiferromagnetic impurity phases. Recent studies on Pauli-paramagnetic LaFePO [87] revealed Fe_2P (T_C = 266 K [97]) and $FeSn_2$ (T_N = 380 K [98]) as minor by-products. Especially ferromagnetic Fe_2P might influence the superconducting transition temperature (*vide infra*).

Table 2. Magnetic properties of various ZrCuSiAs-type compounds.

Compound	magnetism	μ_{exp} (μ_B)	T_N, T_C (K)	Θ (K)	Ref.
Pnictides					
LaMnPO	F	–	320	–	[33]
LaZnPO	D	–	–	–	[64]
CeFePO	P	2.56	–	−52	[48]
LaCoPO	F	–	43	–	[46]
'SmCoP'	F	1.36(3)	85(4)	115(3)	[21]
UCuPO	AF	2.68	220	–	[13]
CeRuPO	F	2.3	15	8	[51]
CeOsPO	AF	2.45	4.5	−9	[51]
LaCoAsO	F	–	66	–	[46]
LaZnAsO	D	–	–	–	[64]
CeZnAsO	P	2.52	–	–	[64]
PrZnAsO	P	3.58	–	–	[64]
NdZnAsO	P	3.45	–	–	[64]
LaZnSbO	D	–	–	–	[64]
CeZnSbO	P	2.43	–	–	[64]
CeZnSbO	P	2.37	–	−14.1	[95]
PrZnSbO	P	3.28	–	−18.3	[95]
NdZnSbO	P	3.33	–	–	[64]
Chalcogenides					
LaCuSO	D	–	–	–	[96]
CeCuSO	IV	1.62	–	−5.3	[83]
	P	2.1	–	–	[79]
$CeCu_{0.8}SO$	P	2.13(6)	–	−30.2(1)	[40]
PrCuSO	P	3.5	–	–	[96]
	P	3.1	–	–	[79]
NdCuSO	P	3.7	–	–	[96]
	P	3.3	–	–	[79]
CeAgSO	P	2.10(1)	–	−28.1(3)	[40]
LaCuTeO	D	–	–	–	[75]
Hydrides					
CeCoSiH	SF	2.72(5)	–	−56(1)	[37]
CeCoGeH	SF	2.78(5)	–	−29(1)	[68]
CeRuSiH	AF	2.59(3)	7.5(2); 3.1(2)	−18	[70]

D: diamagnetism; P: paramagnet, AF: antiferromagnet, F: ferromagnet, SF: spin fluctuation; IV: intermediate valence; T_N: Néel temperature, T_C: Curie temperature, μ_{exp}: experimental magnetic moment, Θ: paramagnetic Curie temperature (Weiss constant).

Several cerium-based compounds were studied in detail with respect to their magnetic behavior. CeZnAsO [64], CeZnSbO [64, 95], CeCuSO [40, 79, 83], and CeAgSO [40] are paramagnetic down to low temperatures without indications for magnetic ordering. Except CeCuSO, the experimentally determined magnetic moments are close to the free-ion value of 2.54 μ_B for Ce^{3+}. Takano *et al.* [83] recently reported that CeCuSO has a magnetic moment of only 1.62 μ_B per formula unit, much smaller than the free-ion value, indicating intermediate-valent

cerium. Specific heat measurements show a γ value of about 324 mJ mol^{-1}K^{-2}, pointing to heavy Fermion character. This is also supported by results of resistivity measurements. Independent susceptibility measurements by Ueda *et al*. [79] and Chan *et al*. [40] revealed higher magnetic moments of 2.1 μ_B and furthermore, significant copper defects have been reported for $CeCu_{1-x}SO$ [39, 79] which certainly strongly influence the magnetic behavior. Further investigations on this system are necessary in order to understand the magnetic and electronic behavior in more detail.

The intermediate cerium valence of several of the cerium based compounds was already evident from the plots of the cell volumes [39, 49, 79]. In view of these negative deviations of the cell volumes from the Iandelli plots it is interesting that the experimentally observed magnetic moment of CeFePO of 2.56 μ_B is even slightly higher than the free-ion value [48]. CeFePO is a magnetically non-ordered heavy Fermion metal with a Kondo temperature of 10 K and a γ value of 700 mJ mol^{-1}K^{-2}. In contrast, ferromagnetic ordering at T_C = 15 K has been observed for CeRuPO [51], while LaRuPO is non-magnetic and behaves like a classical metal without anomalies down to 0.5 K. CeRuPO is a rare example of a ferromagnetic Kondo lattice system. The closely related compound CeOsPO orders antiferromagnetically at T_N = 4.5 K, and the magnetic ordering temperature decreases with increasing field strength.

A much higher ordering temperature of 85(4) K has been observed for SmCoPO, originally reported as 'SmCoP' [21]. This behavior has been ascribed to the ferromagnetic ordering of the cobalt magnetic moments. For the paramagnetic range, a moment of 1.36(3) μ_B per Co atom was deduced. UCuPO [13] has an even higher magnetic ordering temperature. The uranium magnetic moments show antiferromagnetic alignment below the Néel temperature of 220(2) K.

PrZnAsO, NdZnAsO [64], PrZnSbO [95], NdZnSbO [64], PrCuSO, and NdCuSO [79, 96] contain stable trivalent praseodymium and neodymium. The experimentally determined magnetic moments are in agreement with the corresponding free-ion values. All of these samples did not show magnetic ordering down to low temperatures (usually 4.2 K). The susceptibilities of PrCuSO and NdCuSO deviate from a simple Curie-Weiss law due to crystal field effects. The corresponding crystal field parameters have been determined by Nakao *et al*. [96] using an operator equivalent method.

The arsenide oxide LaFeAsO shows a spin-density-wave instability around 150 K which is associated with an abrupt structural distortion [54, 55]. The latter is associated with long-range antiferromagnetic ordering below *ca.* 134 K [55]. Evidence for the structural distortion was obtained from high-resolution neutron powder and synchrotron X-ray diffraction experiments. While de la Cruz *et al.* [55] suggest a symmetry reduction directly to the monoclinic system (space group $P112/n$, but with constrained lattice parameters a and b), Nomura *et al.* [54] propose a symmetry reduction to the orthorhombic system, space group *Cmma*. On the basis of crystallographic group-subgroup relations [99 – 101] we consider the latter symmetry reduction as more probable since it is a simple *translationengleiche* transition of index 2 (t2) from $P4/nmm$ to *Cmma* with a cell transformation $a + b$, $a - b$, c. In this way the a and b parameters of the superstructure cell are decoupled, and indeed one observes smaller a and larger b parameters in the ordered state [54]. The symmetry reduction to the monoclinic system requires at least two steps, and the constraints on the lattice parameters [55] are questionable.

A very interesting situation occurs for the quaternary hydrides CeCoSiH [37], CeMnGeH, CeFeSiH, CeCoGeH [68, 102, 103], and CeRuSiH [70, 88], which were obtained through hydrogenation of the ternary intermetallic silicides and germanides. This is in contrast to all other ZrCuSiAs-type compounds, which are only stable as quaternary variants. Hydrogenation of the antiferromagnetic compounds CeCoSi and CeCoGe leads to spin fluctuation behavior in CeCoSiH and CeCoGeH [102, 103]. In the sequence CeMnGe $\rightarrow$ CeMnGeH the magnetic ordering of the cerium substructure is suppressed [71]. The temperature dependence of the magnetization of CeMnGeH is characteristic of a ferromagnetic, ferrimagnetic, or canted magnetic system. Two ordering temperatures, T_{N_1} = 313(2) and T_{N_2} = 41(2) K, have been observed. In the sequence CeRuSi $\rightarrow$ CeRuSiH, hydrogenation changes the moderate heavy Fermion system to an antiferromagnet (the hydrogen insertion diminishes the influence of the Kondo effect) with two ordering temperatures, T_{N1} = 7.5(2) and T_{N2} = 3.1(2) K [70, 88]. The hydrogen content of LaCoGeH was proven by ^{1}H MAS NMR [102].

Superconductivity

The first report on superconductivity in the ZrCuSiAs-type compound LaFePO was published in

2006 [25]. Even though it appeared remarkable to find superconductivity in an iron compound, the transition temperature (T_C) of 3.5 K was not spectacular at that time. The same holds true for LaNiPO, which becomes superconducting at 4.5 K [26, 27]. The transition temperature of phase-pure LaFePO is probably higher because of the presence of ferromagnetic impurities in the samples (Fe, Fe_2P). Those can reduce T_C due to the permanent magnetic field inside the sample. By treating finely ground LaFePO with a magnet under liquid N_2, it is possible to remove most of those impurities and to increase T_C from 3.5 to 7 K. [87].

The breakthrough came in February 2008, when Kamihara reported superconductivity at 26 K in $LaFeAs(O_{1-x}F_x)$ [28]. Then Chinese groups took over, and even higher T_C values followed quickly. By replacing the lanthanum ions with smaller rare earth ions, the T_C increases strongly to 41 K in $CeFeAs(O_{1-x}F_x)$, 52 K in $PrFeAs(O_{1-x}F_x)$ and $NdFeAs(O_{1-x}F_x)$ and reaches 55 K in $SmFeAs(O_{1-x}F_x)$ [104]. These transition temperatures can be regarded as lower limits, because of occasional poor sample quality. $LaFeAs(O_{1-x}F_x)$ samples synthesized under high pressure [105] showed superconductivity at 41 K instead of 26 K. The authors argued that the reason is a slightly smaller lattice parameter. However, the difference is very small, and this seems unlikely to be the origin of this enormous increase of T_C. Moreover, the true fluoride content of the doped materials is unknown up to now. Most of the so far published *RE*$FeAs(O_{1-x}F_x)$ compounds contain significant amounts of impurity phases, among them *RE*OF, which makes the true content of fluoride inside the structure unreliable. This is supported by the finding that fluoride-free, but oxygen-deficient compounds *RE*$FeAsO_{1-x}$ become also superconducting between 30 and 55 K [61].

The undoped parent compound LaFeAsO is not superconducting, but shows distinctive anomalies of the physical properties around 150 K. The electrical resistivity and magnetic susceptibility drop at this temperature as a consequence of a structural phase transition [54, 55] (*vide ultra*). The latter has been assigned to the lock-in of a spin density wave (SDW) into long-range antiferromagnetic ordering. The correlation between the structural and magnetic transition was also proved by ^{57}Fe Mössbauer spectroscopy [106, 107] (*vide infra*).

The structural and magnetic phase transition of LaFeAsO is successively suppressed by increasing doping with electrons or holes. Doped materials like $LaFeAsO_{0.85}F_{0.15}$ (nominal) show no splitting of the ^{57}Fe Mössbauer signal, thus the magnetic ordering is also suppressed. Superconductivity emerges upon adding or removing 0.1 – 0.2 electrons per formula unit. It is generally believed that the nature of the SDW transition in undoped LaFeAsO is one major key to understand superconductivity in iron arsenides, and that the SDW seems to be mandatory for higher transition temperatures. Indeed, this may be the reason for the low critical temperatures of the isostructural and isoelectronic phosphides *RE*FePO, where the SDW transition is not observed [87].

But even though several uncertainties, among them the role of the SDW transition as well as the exact chemical composition of the superconducting phases, still exist, the new ZrCuSiAs-type superconductors have heralded a new age of superconductivity research. Bulk superconductivity at critical temperatures above 50 K has not been observed since the discovery of the cuprate superconductors by Bednorz and Müller, more than twenty years ago [108]. Even if the pnictide oxide materials have not (yet) reached such high T_C, their discovery will undoubtedly give a fresh impetus to the great issue of superconductivity, namely the still open question about the mechanism of Cooper pair formation at temperatures well above 40 K. Actually, more than twenty theories related more or less to the classical BCS theory of 1957, have not yet been able to explain the coupling of the conduction electrons in these material conclusively [109].

Some properties of the ZrCuSiAs-type superconductors show similarities to those of the cuprates. In both cases, non-superconducting antiferromagnetic parent structures exist. These are La_2CuO_4 in the case of the cuprates and LaFeAsO in the case of the pnictide oxides. Upon doping with holes or electrons, the antiferromagnetic state becomes unstable, and superconductivity emerges. But there are also differences. La_2CuO_4 is an insulator, but LaFeAsO is a poor metal at r. t. This is due to direct orbital interactions between the iron atoms at distances of 285 pm, whereas no direct *d* orbital overlap occurs in the cuprates of the La_2CuO_4 family.

Optical and opto-electronic properties

Depending on the transition metal and group V / VI component, the various ZrCuSiAs-type compounds show different color. The dimorphic (tetragonal ZrCuSiAs-type low-, and rhombohedral NdZnPO-type

high-temperature modification) *RE*ZnPO phosphide oxides are transparent with light-yellow to dark-red color [22, 23]. According to these relatively large band gaps, the model of ionic formula splitting discussed above is best applicable to these compounds. Single crystal absorption spectra measured for *RE*ZnPO (*RE* = Y, La, Pr, Nd, Sm, Dy) in the nir/vis region reveal unexpected variations for the optical band gap of these phosphide oxides. For *RE* = Pr, Nd, Sm, Dy, and Ho f-f electronic transitions with well-resolved ligand-field splittings are observed in the range 6000 – 20000 cm^{-1}. DFT band structure calculations show similarity between the valence bands of tetragonal and rhombohedral *RE*ZnPO which possess mainly P-3p character. In both cases, the conduction bands have mainly Zn-4s character, but a significant contribution of *RE*-5d occurs in rhombohedral *RE*ZnPO, which is responsible for a smaller optical band gap for the latter compounds. Variations of the energy gaps of tetragonal *RE*ZnPO can be explained by hybridization of Zn-4s + *RE*-5d + *RE*-4f orbitals for the conduction band.

With the heavier group V and group VI elements, the band gaps become smaller, and the compounds are black. Some of them are even metallic. To give an example, experimental data show optical band gaps of $E_g < 0.73$ and 0.71 eV for the black compounds $CeCu_{0.8}SO$ (p-type semiconductor) and CeAgSO at 298 K, respectively [40]. These values compare well with the results of electronic structure calculations. The experimental optical band gaps for LaCuTeO and NdCuTeO are 2.31 and 2.26 eV, respectively [41]. According to positive values of the Seebeck and Hall coefficients, these compounds have p-type semiconductivity. Electronic structure calculations of these materials have revealed that the larger dispersion of the Cu 3d orbitals and the presence of Te 5p states near the valence band maximum (VBM) are responsible for the larger hole mobility of LaCuTeO as compared to LaCuSeO and LaCuSO.

The full ionic formula splitting is also valid for the fluoride sulfides. Grossholz and Schleid [45] observed emerald-green color for the platelet-shaped crystals of EuCuSF. Also SmCuSeF [74] shows deep color, while the fluoride BaZnPF [36] is brownish, indicating a smaller band gap. Upon doping, p-type semiconductivity occurs for the solid solutions $Sr_{1-x}Na_xCuSF$ and $SrCuSO_xF_{1-x}$ [73].

Besides the studies of recently discovered superconductivity in the pnictide oxides, the so far broadest investigations for ZrCuSiAs-type materials were performed for the oxysulfides [12]. In their first report Ueda *et al.* [11] studied $La_{1-x}Sr_xCuSO$ (x = 0, 0.05) thin films prepared by radio-frequency sputtering [110] which showed high optical transmission of $> 70\,\%$ in the visible and near-infrared region and an energy gap of 3.1 eV. These materials are p-type semiconductors with a sharp photoluminescence peak at the optical absorption edge. The investigations have also been extended to include other diamagnetic rare earth elements, *i. e.* YCuSeO and LaCuSeO [86].

The widegap oxychalcogenides LaCu*Ch*O (*Ch* = chalcogen) are an outstanding family of materials, since widegap p-type conduction is rather difficult to realize. Furthermore, these materials exhibit high hole mobility, degenerate p-type conduction, r. t. exciton properties, and large third order optical nonlinearity. All these highly interesting features have been summarized recently in a review by Hiramatsu *et al.* [12]. These authors also discuss a first application. It is possible to run a blue light-emitting diode at r. t. using an *pn* hetero-junction composed of an LaCuSO epilayer and an n-type amorphous $InGaZn_5O_8$ [12].

The concentration of lattice imperfections is an important parameter influencing the optical properties and the conduction behavior. Takase *et al.* [111] treated bars of LaCuSO under different thermal conditions, *i. e.* (a) 1070 K for 6 h, (b) 1170 K for 6 h, and (c) 1170 K for 40 h. An increase of lattice imperfections (evident also from the X-ray powder data) was found to increase the intensity of the wide emission bands, and drastically decrease the specific resistivity with increasing annealing time. Another important parameter determining the resistivity behavior is doping. Koyano *et al.* [85] studied the whole series $(La_{1-x}Ca_x)Cu_{1-x}T_xSO$ (T = Mn, Co, Ni, Zn). Small changes in the interlayer distances shift the specific resistivity by several decades.

So far, ionic conductivity has only been reported for LaAgSO [8]. The single crystal X-ray data [9] revealed an enlarged displacement parameter for the silver atoms, although refinement of the occupancy parameters showed full occupancy. Electrochemical measurements with a cell $^{+}$Ag/LaAgSO/Pt^{-} showed essentially ionic conductivity in the temperature regime 298 to 523 K with an activation energy of 0.195 eV. Considering the defects on the transition metal sites of other copper and silver containing *RE*CuSO and *RE*AgSO compounds (*vide ultra*), one can also expect some copper and silver mobility in these materials.

Mössbauer spectroscopy

The three iron-based compounds LaFePO [87], LaFeAsO and $LaFeAsO_{0.89}F_{0.11}$ [106, 107] have been characterized by temperature dependent ^{57}Fe Mössbauer spectroscopy. Spectra of LaFePO at 298, 77, 4.2 and 4 K showed single signals at isomer shift values around 0.35 mm s^{-1}, subject to weak quadrupole splitting [87]. At 4 K, a symmetric line broadening appears, resulting from a small transferred magnetic hyperfine field of 1.15(1) T, accompanied by an angle of 54.7(5)° between B_{hf} and V_{zz}, the main component of the electric field gradient tensor.

The different electronic states of iron in LaFeAsO and fluoride-doped $LaFeAsO_{0.89}F_{0.11}$ were studied in detail by ^{57}Fe Mössbauer spectroscopy [106, 107]. The ^{57}Fe spectra proved spin ordering in LaFeAsO and its suppression upon doping. The isomer shifts of the arsenide oxides are close to the data observed for the phosphides. Below the antiferromagnetic ordering (T_N = 138 K), LaFeAsO shows full magnetic hyperfine field splitting with a hyperfine field of 4.86 T [106]. The magnetic moment at the iron atoms was estimated to be in the range 0.25 – 0.35 μ_B per Fe atom.

The *RE*MnSbO (*RE* = La, Ce, Pr, Nd, Sm, Gd) and *RE*ZnSbO (*RE* = La, Ce, Pr) antimonide oxides were also studied *via* ^{121}Sb Mössbauer spectroscopy [34]. In agreement with the crystal structure, all antimonides show single signals at isomer shifts ranging from −7.82 (LaMnSbO) to −8.37 mm s^{-1} (PrZnSbO). According to the ionic formula splitting discussed above the *RE*TSbO compounds contain Sb^{3-} pnictide anions. This Zintl anion also occurs in the alkali metal antimonides A_3Sb (*A* = Li, Na, K, Rb) with comparable isomer shifts of −7.3 mm s^{-1} for Li_3Sb [112] and −8.39 mm s^{-1} for Rb_3Sb [113]. The III-V semiconductors AlSb, GaSb and InSb [114] also show comparable isomer shifts. Thus, the ^{121}Sb Mössbauer spectroscopic data clearly underline the antimonide character.

Conclusions and Outlook

So far, more than 150 representatives with the tetragonal ZrCuSiAs-type structure (tP8) are known. These materials have intensively been investigated in the last 15 years with respect to their highly interesting physical properties: (i) the chalcogenides LaCu*Ch*O are widegap semiconductors with unique optoelectronic properties and with substantial potential for LED application and optoelectronic devices, (ii) compounds like the ferromagnetic Kondo system CeRuPO are highly attractive materials for basic research, and (iii) several of the pnictide oxides have outstanding superconducting properties. In view of the rapidly growing work in this new research field (several new contributions are published daily on the preprint server (arXiv.org) of the Cornell University Library) we can expect further interesting results in the near future.

Acknowledgement

This work was financially supported by the Deutsche Forschungsgemeinschaft.

[1] V. Johnson, W. Jeitschko, *J. Solid State Chem.* **1974**, *11*, 161.
[2] H. Sprenger, *J. Less-Common Met.* **1974**, *34*, 39; L. S. Andrukhiv, L. O. Lysenko, Ya. P. Yarmolynk, E. I. Gladyshevskii, *Dopov. Akad. Nauk. Ukr., Ser. A* **1975**, 645.
[3] F. Jellinek, H. Hahn, *Naturwissenschaften* **1962**, *49*, 103.
[4] A. J. Klein Haneveld, F. Jellinek, *Rec. Trav. Chim.* **1964**, *83*, 776.
[5] V. Johnson, W. Jeitschko, *J. Solid State Chem.* **1973**, *6*, 306.
[6] P. Villars, L. D. Calvert, *Pearson's Handbook of Crystallographic Data for Intermetallic Phases* (2nd Edition), American Society for Metals, Materials Park, O. H, **1991**, and desk edition, **1997**.
[7] W. B. Pearson, *Z. Kristallogr.* **1985**, *171*, 23.
[8] M. Palazzi, C. Carcaly, J. Flahaut, *J. Solid State Chem.* **1980**, *35*, 150.
[9] M. Palazzi, S. Jaulmes, *Acta Crystallogr.* **1981**, *B37*, 1337.
[10] P. Palazzi, *C. R. Acad. Sc. Ser. II* **1981**, *292*, 789.
[11] K. Ueda, S. Inoue, S. Hirose, H. Kawazoe, H. Hosono, *Appl. Phys. Lett.* **2000**, *77*, 2701.
[12] H. Hiramatsu, H. Kamioka, K. Ueda, H. Ohta, T. Kamiya, M. Hirano, H. Hosono, *Phys. Stat. Sol. A* **2006**, *203*, 2800.
[13] D. Kaczorowski, J. H. Albering, H. Noël, W. Jeitschko, *J. Alloys Compd.* **1994**, *216*, 117.
[14] B. I. Zimmer, W. Jeitschko, J. H. Albering, R. Glaum, M. Reehuis, *J. Alloys Compd.* **1995**, *229*, 238.
[15] J. H. Albering, W. Jeitschko, *Z. Naturforsch.* **1996**, *51b*, 257.
[16] A. T. Nientiedt, B. I. Zimmer, P. Wollesen, W. Jeitschko, *Z. Kristallogr.* **1996**, *Suppl. 11*, 101.

[17] P. Wollesen, J. W. Kaiser, W. Jeitschko, *Z. Naturforsch.* **1997**, *52b*, 1467.
[18] A. T. Nientiedt, W. Jeitschko, P. G. Pollmeier, M. Brylak, *Z. Naturforsch.* **1997**, *52b*, 560.
[19] A. T. Nientiedt, W. Jeitschko, *Inorg. Chem.* **1998**, *37*, 386.
[20] P. Quebe, L. J. Terbüchte, W. Jeitschko, *J. Alloys Compd.* **2000**, *302*, 70.
[21] M. Reehuis, W. Jeitschko, *J. Phys. Chem. Solids* **1990**, *51*, 961.
[22] H. Lincke, T. Nilges, R. Pöttgen, *Z. Anorg. Allg. Chem.* **2006**, *632*, 1804.
[23] H. Lincke, R. Glaum, V. Dittrich, M. Tegel, D. Johrendt, W. Hermes, M. H. Möller, T. Nilges, R. Pöttgen, *Z. Anorg. Allg. Chem.* **2008**, *634*, 1339.
[24] B. I. Zimmer, *Darstellung und Charakterisierung ternärer Phosphide und quaternärer Phosphid-Oxide der Seltenerdelemente und des Thoriums mit Übergangsmetallen*, Dissertation, Universität Münster, Münster, **1996**.
[25] Y. Kamihara, H. Hiramatsu, M. Hirano, R. Kawamura, H. Yanagi, T. Kamiya, H. Hosono, *J. Am. Chem. Soc.* **2006**, *128*, 10012.
[26] T. Watanabe, H. Yanagi, T. Kamiya, Y. Kamihara, H. Hiramatsu, M. Hirano, H. Hosono, *Inorg. Chem.* **2007**, *46*, 7719.
[27] M. Tegel, D. Bichler, D. Johrendt, *Solid State Sci.* **2008**, *10*, 193.
[28] Y. Kamihara, T. Watanabe, M. Hirano, H. Hosono, *J. Am. Chem. Soc.* **2008**, *130*, 3296.
[29] Z.-A. Ren, J. Yang, W. Lu, W. Yi, G.-C. Che, X.-L. Dong, L.-L. Sun, Z.-X. Zhao, *Mater. Res. Innov.* **2008**, *12*, 1.
[30] D. Johrendt, R. Pöttgen, *Angew. Chem.* **2008**, *120*, 4960; *Angew. Chem. Int. Ed.* **2008**, *47*, 4782.
[31] M. G. Kanatzidis, R. Pöttgen, W. Jeitschko, *Angew. Chem.* **2005**, *117*, 7156; *Angew. Chem. Int. Ed.* **2005**, *44*, 6996.
[32] C. Krellner, C. Geibel, *J. Cryst. Growth* **2008**, *310*, 1875.
[33] E. Motomitsu, M. Hirano, H. Yanagi, T. Kamiya, H. Hosono, *Jpn. J. Appl. Phys.* **2005**, *44*, L1344.
[34] I. Schellenberg, T. Nilges, R. Pöttgen, *Z. Naturforsch.* **2008**, *63b*, 834.
[35] H. Kabbour, L. Cario, F. Boucher, *J. Mater. Chem.* **2005**, *15*, 3525.
[36] L. Cario, H. Kabbour, A. Meerschaut, *Chem. Mater.* **2005**, *17*, 234.
[37] B. Chevalier, S. F. Matar, *Phys. Rev. B* **2004**, *70*, 174408.
[38] W. J. Zhu, Y. Z. Huang, C. Dong, Z. X. Zhao, *Mater. Res. Bull.* **1994**, *29*, 143.
[39] D. O. Charkin, A. V. Akopyan, V. A. Dolgikh, *Russ. J. Inorg. Chem.* **1999**, *44*, 833.
[40] G. H. Chan, B. Deng, M. Bertoni, J. R. Ireland, M. C. Hersam, T. O. Mason, R. P. Van Duyne, J. A. Ibers, *Inorg. Chem.* **2006**, *45*, 8264.
[41] M. L. Liu, L. B. Wu, F. Q. Huang, L. D. Chen, J. A. Ibers, *J. Solid State Chem.* **2007**, *180*, 62.
[42] Y. Takano, C. Ogawa, Y. Miyahara, H. Ozaki, K. Sekizawa, *J. Alloys Compd.* **1997**, *249*, 221.
[43] W. C. Sheets, E. S. Stampler, H. Kabbour, M. I. Bertoni, L. Cario, Th. O. Mason, T. J. Marks, K. R. Poeppelmeier, *Inorg. Chem.* **2007**, *46*, 10741.
[44] H. Hiramatsu, H. Yanagi, T. Kamiya, K. Ueda, M. Hirano, H. Hosono, *Chem. Mater.* **2008**, *20*, 326.
[45] H. Grossholz, Th. Schleid, *Z. Kristallogr.* **2002**, *Suppl. 19*, 104.
[46] H. Yanagi, R. Kawamura, T. Kamiya, Y. Kamihara, M. Hirano, T. Nakamura, H. Osawa, H. Hosono, *Phys. Rev. B* **2008**, *77*, 224431.
[47] T. M. McQueen, M. Regulacio, A. J. Williams, Q. Huang, J. W. Lynn, Y. S. Hor, D. V. West, M. A. Green, R. J. Cava, *Phys. Rev. B* **2008**, *78*, 024521.
[48] E. M. Brüning, C. Krellner, M. Baenitz, A. Jesche, F. Steglich, C. Geibel, *ArXiv.org, e-Print Archive, Condensed Matter* **2008**, 0804.3250.
[49] W. Jeitschko, B. I. Zimmer, R. Glaum, L. Boonk, U. Ch. Rodewald, *Z. Naturforsch.* **2008**, *63b*, 934.
[50] K. Kayanuma, H. Hiramatsu, M. Hirano, R. Kawamura, H. Yanagi, T. Kamiya, H. Hosono, *Phys. Rev. B* **2007**, *76*, 195325.
[51] C. Krellner, N. S. Kini, E. M. Brüning, K. Koch, H. Rosner, M. Nicklas, M. Baenitz, C. Geibel, *Phys. Rev. B* **2007**, *76*, 104418.
[52] C. Y. Liang, R. C. Che, H. X. Yang, H. F. Tian, R. J. Xiao, J. B. Lu, R. Li, J. Q. Li, *Supercond. Sci. Technol.* **2007**, *20*, 687.
[53] T. Watanabe, H. Yanagi, Y. Kamihara, T. Kamiya, M. Hirano, H. Hosono, *J. Solid State Chem.* **2008**, *181*, 2117.
[54] T. Nomura, S. W. Kim, Y. Kamihara, M. Hirano, P. V. Sushko, K. Kato, M. Takata, A. L. Shluger, H. Hosono, *ArXiv.org*, *e-Print Archive, Condensed Matter* **2008**, 0804.3569.
[55] C. De la Cruz, Q. Huang, J. W. Lynn, J. Li, W. Ratcliff, L. L. Zarestky, H. A. Mook, G. F. Chen, J. L. Luo, N. L. Wang, P. Dai, *Nature* **2008**, *453*, 899.
[56] X. H. Chen, T. Wu, G. Wu, R. H. Liu, H. Chen, D. F. Fang, *ArXiv.org, e-Print Archive, Condensed Matter* **2008**, 0803.3603.
[57] G. F. Chen, Z. Li, G. Li, J. Zhou, J. Dong, W. Z. Hu, P. Zheng, Z. J. Chen, J. L. Luo, N. L. Wang, *Phys. Rev. Lett.* **2008**, *101*, 057007.
[58] W. Lu, J. Yang, X. L. Dong, Z. A. Ren, G. C. Che, Z. X. Zhao, *New J. Phys.* **2008**, *10*, 063026.
[59] G. F. Chen, Z. Li, D. Wu, G. Li, W. Z. Hu, J. Dong,

P. Zheng, J. L. Luo, N. L. Wang, *Phys. Rev. Lett.* **2008**, *100*, 247002.
[60] P. Cheng, L. Fang, H. Yang, X. Zhu, G. Mu, H. Luo, Z. Wang, H.-H. Wen, *Science in China G* **2008**, *51*, 719.
[61] Z.-A. Ren, W. Lu, J. Yang, W. Yi, X.-L. Chen, Z.-C. Li, G.-C. Che, X.-L. Dong, L.-L. Sun, F. Zhou, Z.-X. Zhao, *Europhys. Lett*. **2008**, *83*, 17002.
[62] H.-H. Wen, G. Mu, L. Fang, H. Yang, X. Zhu, *EPL* **2008**, *82*, 17009.
[63] M. A. McGuire, A. D. Christianson, A. S. Sefat, R. Jin, E. A. Payzant, B. C. Sales, M. D. Lumsden, D. Mandrus, *ArXiv.org, e-Print Archive, Condensed Matter* **2008**, 0804.0796.
[64] Y. Takano, S. Komatsuzaki, H. Komasaki, T. Watanabe, Y. Takahashi, K. Takase, *J. Alloys Compd*. **2008**, *451*, 467.
[65] V. L. Kozhevnikov, O. N. Leonidova, A. L. Ivanovskii, I. R. Shein, B. N. Goshchitskii, A. E. Karkin, *ArXiv.org, e-Print Archive, Condensed Matter* **2008**, 0804.4546.
[66] M. Tegel, D. Johrendt, *Z. Anorg. Allg. Chem*. **2008**, *634*, in press.
[67] H. Abe, K. Yoshii, *J. Solid State Chem*. **2002**, *165*, 372.
[68] B. Chevalier, E. Gaudin, F. Weill, J.-L. Bobet, *Intermetallics* **2004**, *12*, 437.
[69] J.-L. Bobet, M. Pasturel, B. Chevalier, *Intermetallics* **2006**, *14*, 544.
[70] B. Chevalier, E. Gaudin, S. Tencé, B. Malaman, J. Rodriguez Fernandez, G. André, B. Coqblin, *Phys. Rev. B* **2008**, *77*, 014414.
[71] B. Chevalier, M. Pasturel, J.-L. Bobet, O. Isnard, *Solid State Commun*. **2005**, *134*, 529.
[72] W. J. Zhu, Y. Z. Huang, F. Wu, C. Dong, H. Chen, Z. X. Zhao, *Mater. Res. Bull*. **1994**, *29*, 505.
[73] H. Kabbour, L. Cario, S. Jobic, B. Corraze, *J. Mater. Chem*. **2006**, *16*, 4165.
[74] H. Grossholz, Th. Schleid, *Z. Anorg. Allg. Chem*. **2002**, *628*, 2169.
[75] Y. Ohki, K. Takase, Y. Takahashi, Y. Takano, K. Sekizawa, *J. Alloys Compd*. **2006**, *408 – 412*, 98.
[76] P. S. Berdonosov, A. M. Kusainova, L. N. Kholodkovskaya, V. A. Dolgikh, L. G. Akselrud, B. A. Popovkin, *J. Solid State Chem*. **1995**, *118*, 74.
[77] T. Ohtani, M. Hirose, T. Sato, K. Nagaoka, M. Ibawe, *Jpn. J. Appl. Phys*. **1993**, *32 (Suppl. 32-3)*, 316.
[78] D. O. Charkin, P. S. Berdonosov, V. A. Dolgikh, P. Lightfoot, *J. Alloys Compd*. **1999**, *292*, 118.
[79] K. Ueda, K. Takafuji, H. Hosono, *J. Solid State Chem*. **2003**, *170*, 182.
[80] D. O. Charkin, P. S. Berdonosov, V. A. Dolgikh, P. Lightfoot, *Russ. J. Inorg. Chem*. **2000**, *45*, 182.
[81] B. Popovkin, A. M. Kusainova, V. A. Dolgikh, L. G. Akselrud, *Russ. J. Inorg. Chem*. **1998**, *43*, 1471.
[82] A. M. Kusainova, P. S. Berdonosov, L. G. Akselrud, L. N. Kholodkovskaya, V. A. Dolgikh, B. A. Popovkin, *J. Solid State Chem*. **1994**, *112*, 189.
[83] Y. Takano, H. Nakao, Y. Takahashi, K. Takase, S. Misawa, J. Clarke, C. F. Smura, K. Sekizawa, *J. Alloys Compd*. **2006**, *408 – 412*, 101.
[84] P. Lauxmann, T. Schleid, *Z. Anorg. Allg. Chem*. **2000**, *626*, 2253.
[85] S. Koyano, K. Takase, Y. Kuroiwa, S. Aoyagi, O. Shoji, K. Sato, Y. Takahashi, Y. Takano, K. Sekizawa, *J. Alloys Compd*. **2006**, *408 – 412*, 95.
[86] K. Ueda, K. Takafuji, H. Yanagi, T. Kamiya, H. Hosono, H. Hiramatsu, M. Hirano, N. Hamada, *J. Appl. Phys*. **2007**, *102*, 113714.
[87] M. Tegel, I. Schellenberg, R. Pöttgen, D. Johrendt, *Z. Naturforsch*. **2008**, *63b*, 1057.
[88] S. Tencé, G. André, E. Gaudin, B. Chevalier, *J. Phys.: Condens. Matter* **2008**, *20*, 255239.
[89] S. Lebègue, *Phys. Rev. B* **2007**, *75*, 035110.
[90] S.-I. Inoue, K. Ueda, H. Hosono, N. Hamada, *Phys. Rev. B* **2001**, *64*, 245211.
[91] Z. P. Yin, S. Lebègue, M. J. Han, B. Neal, S. Y. Savrasov, W. E. Pickett, *Phys. Rev. Lett.* **2008**, *101*, 047001.
[92] D. J. Singh, M.-H. Du, *Phys. Rev. Lett.* **2008**, *100*, 237003.
[93] I. I. Mazin, D. J. Singh, M. D. Johannes, M. H. Du, *Phys. Rev. Lett.* **2008**, *101*, 057003.
[94] T. Yildirim, *Phys. Rev. Lett.* **2008**, *101*, 057010.
[95] S. Komatsuzaki, Y. Ohki, M. Sasaki, Y. Takahashi, K. Takase, Y. Takano, K. Sekizawa, *AIP Conf. Proc*. **2006**, *850*, 1255.
[96] H. Nakao, Y. Takano, K. Takase, K. Sato, S. Hara, S. Ikeda, Y. Takahashi, K. Sekizawa, *J. Alloys Compd*. **2006**, *408 – 412*, 104.
[97] A. J. P. Meyer, M. C. Cadeville, *J. Phys. Soc. Jpn*. **1962**, *17*, 223.
[98] K. Kanematsu, K. Yasukochi, T. Ohoyama, *J. Phys. Soc. Jpn*. **1960**, *15*, 2358.
[99] H. Bärnighausen, *MATCH, Commun. Math. Chem*. **1980**, *9*, 139.
[100] U. Müller, *Z. Anorg. Allg. Chem*. **2004**, *630*, 1519.
[101] H. Wondratschek, U. Müller, *International Tables for Crystallography A1: Symmetry relations between space groups*, Kluwer Academic Publishers, Dordrecht, **2004**.
[102] B. Chevalier, S. F. Matar, J. Sanchez Marcos, J. Rodriguez Fernandez, *Physica B* **2006**, *378 – 380*, 795.
[103] B. Chevalier, S. F. Matar, M. Ménétrier, J. Sanchez Marcos, J. Rodriguez Fernandez, *J. Phys.: Condens. Matter* **2006**, *18*, 6045.
[104] Z.-A. Ren, W. Lu, J. Yang, W. Yi, X.-L. Shen, Z.-C. Li, G.-C. Che, X.-L. Dong, L.-L. Sun, F. Zhou, Z.-X. Zhao, *Chin. Phys. Lett*. **2008**, *25*, 2215.

[105] W. Lu, X.-L. Shen, J. Yang, Z.-C. Li, W. Yi, Z.-A. Ren, X.-L. Dong, G.-C. Che, L.-L. Sun, F. Zhou, Z.-X. Zhao, *arXiv*:0804.3725.

[106] S. Kitao, Y. Kobayashi, S. Higashitaniguchi, M. Saito, Y. Kamihara, M. Hirano, T. Mitsui, H. Hosono, M. Seto, *ArXiv.org, e-Print Archive, Condensed Matter* **2008**, 0805.0041.

[107] H.-H. Klauss, H. Luetkens, R. Klingeler, C. Hess, F. J. Litterst, M. Kraken, M. M. Korshunov, I. Eremin, S.-L. Drechsler, R. Khasanov, A. Amato, J. Hamann-Borrero, N. Leps, A. Kondrat, G. Behr, J. Werner, B. Büchner, *Phys. Rev. Lett.* **2008**, *101*, 077005.

[108] J. G. Bednorz, K. A. Müller, *Z. Phys. B: Condens. Matter* **1986**, *64*, 189.

[109] A. Cho, *Science* **2006**, *314*, 1072.

[110] H. Hiramatsu, M. Orita, M. Hirano, K. Ueda, H. Hosono, *J. Appl. Phys*. **2002**, *91*, 9177.

[111] K. Takase, M. Koyano, T. Shimizu, K. Makihara, Y. Takahashi, Y. Takano, K. Sekizawa, *Solid State Commun*. **2002**, *123*, 531.

[112] P. E. Lippens, J.-C. Jumas, J. Olivier-Fourcade, *Hyp. Int*. **2004**, *156/157*, 327.

[113] K. Kitadai, M. Takahashi, M. Takeda, *J. Radioanal. Nucl. Chem*. **2003**, *255*, 311.

[114] P. E. Lippens, *Solid State Commun*. **2000**, *113*, 399.